DHI ref. 43/92

Coastal Engineering, 18 (1992) 183–204
Elsevier Science Publishers B.V., Amsterdam

A new form of the Boussinesq equations with improved linear dispersion characteristics. Part 2. A slowly-varying bathymetry

Per A. Madsen and Ole R. Sørensen
Danish Hydraulic Institute, Agern Allé 5, DK-2970 Hørsholm, Denmark

(Received 10 February 1992; accepted after revision 22 June 1992)

ABSTRACT

Madsen, P.A. and Sørensen, O.R., 1992. A new form of the Boussinesq equations with improved linear dispersion characteristics. Part 2. A slowly-varying bathymetry. *Coastal Eng.*, 18: 183–204.

A new form of the Boussinesq equations applicable to irregular wave propagation on a slowly varying bathymetry from deep to shallow water is introduced. The equations incorporate excellent linear dispersion characteristics, and are formulated and solved in two horizontal dimensions. In an earlier paper we concentrated on wave propagation and diffraction on a horizontal bottom in deep water. In this paper these principles are generalized and the Boussinesq equations are extended to include terms proportional to the bottom slope, which are essential for the shoaling properties of the equations. The paper contains a linear shoaling analysis of the new equations and a verification of the numerical model with respect to shoaling and refraction–diffraction in deep and shallow water.

1. INTRODUCTION

The extensive use of the Boussinesq equations to practical studies of wave disturbance in harbours and coastal regions makes it important to establish the range of application of these equations and if possible to improve it. From a theoretical point of view these equations are based on shallow water assumptions but practical problems often require that larger values of the depth to deep water wave length ratios, h/L_0 can be taken into account.

In Part 1 of this work (Madsen et al., 1991a) various classical forms of the Boussinesq equations were discussed and expressions for the corresponding linear dispersion relations were derived and compared to Stokes linear theory. The best form of the classical equations was shown to provide a 5% celerity error for $h/L_0 = 0.22$, which is often taken as the practical deep water limit

Correspondence to: P.A. Madsen, Danish Hydraulic Institute, Agern Allé 5, DK-2970 Hørsholm, Denmark.

0378-3839/92/$05.00 © 1992 Elsevier Science Publishers B.V. All rights reserved.

for these equations. It turns out that a considerable improvement of the accuracy of the linear dispersion relation can be obtained by combining a polynomial expansion of Stokes first order theory with Pade's approximant technique (see also Witting, 1984). In Part 1 we used this technique in combination with the method of operator correspondence to obtain a new set of Boussinesq equations expressed in two horizontal dimensions in terms of the surface elevation and the depth-integrated velocity components. A major improvement of the accuracy of the phase celerity and group velocity was demonstrated, and two-dimensional simulations of wave propagation and diffraction in deep water were performed.

The derivation of the new equations presented in Part 1 neglected all spatial derivatives of the sea bed, and recent analysis (Madsen and Sørensen, 1992) has revealed that for this reason they should not be applied on a variable bathymetry.

In the present paper we shall rederive the new Boussinesq equations including first derivatives of the sea bed (section 2) and make an analysis of the resulting shoaling properties (section 3). It will be demonstrated that for the standard Boussinesq equations the shoaling falsification increases rapidly for h/L_0 exceeding 0.12, and for this reason it must be concluded that on a variable bathymetry the accuracy of the phase celerity generally provides a much too optimistic measure of the practical range of application of the equations (see above). The new equations, on the other hand, provide an excellent accuracy in shoaling as well as in linear dispersion for h/L_0 as large as 0.50 and these equations make it possible to simulate the transformation of irregular wave trains travelling from deep to shallow water. The numerical scheme for the new equations will be described in section 4 and finally the model will be verified with respect to linear shoaling in section 5 and nonlinear refraction–diffraction in section 6.

2. DERIVATION OF THE BOUSSINESQ EQUATIONS

In this section we shall modify the new Boussinesq equations, presented in Part 1 of this work, to include first derivatives of the sea bed. The result will be a set of two-dimensional equations which incorporate excellent linear dispersion characteristics and are valid on a slowly-varying bathymetry.

The starting point for the rederivation will be the classical Boussinesq equations derived by Peregrine (1967) in terms of the depth-averaged velocity components. Formulated in terms of depth-integrated velocities (i.e. fluxes) instead his equations become,

$$S_t + P_x + Q_y = 0 \tag{2.1a}$$

$$P_t+\left(\frac{P^2}{d}\right)_x+\left(\frac{PQ}{d}\right)_y+gdS_x+\psi_1=0 \tag{2.1b}$$

$$Q_t+\left(\frac{Q^2}{d}\right)_y+\left(\frac{PQ}{d}\right)_x+gdS_y+\psi_2=0 \tag{2.1c}$$

where subscripts x, y and t denote differentiation with respect to space and time, d is the total water depth, h is the still water depth, S is the surface elevation, P and Q are the depth-integrated velocity components, and ψ_1 and ψ_2 are the Boussinesq terms defined by

$$\psi_1\equiv\tfrac{1}{6}h^3\left(\left(\frac{P}{h}\right)_{xxt}+\left(\frac{Q}{h}\right)_{xyt}\right)-\tfrac{1}{2}h^2(P_{xxt}+Q_{xyt}) \tag{2.2a}$$

$$\psi_2\equiv\tfrac{1}{6}h^3\left(\left(\frac{Q}{h}\right)_{yyt}+\left(\frac{P}{h}\right)_{xyt}\right)-\tfrac{1}{2}h^2(Q_{yyt}+P_{xyt}) \tag{2.2b}$$

Notice that eqs. (2.2a–b) are expressed in terms of h, which means that nonlinear effects arising from the difference between d and h have been neglected. This makes the formulation different from Abbott et al. (1978). From a consistency point of view such effects are of higher order, and should only be included if they have a positive influence on the simulation of highly nonlinear waves. However, this is not the case and the effect of changing h^2 to hd or d^2 in eqs. (2.2a and b) has been shown to result in an overestimation of the dispersive effects and an underestimation of the crest in solitary waves (see McCowan, 1987).

In the following first derivatives of h will be considered small, and higher derivatives and products of derivatives will consequently be neglected. This leads to the following simplification of eqs. (2.2a and b)

$$\psi_1=-\tfrac{1}{3}h^2(P_{xxt}+Q_{xyt})-\tfrac{1}{6}hh_yQ_{xt}-\tfrac{1}{6}hh_x(2P_{xt}+Q_{yt}) \tag{2.3a}$$

$$\psi_2=-\tfrac{1}{3}h^2(Q_{yyt}+P_{xyt})-\tfrac{1}{6}hh_xP_{yt}-\tfrac{1}{6}hh_y(2Q_{yt}+P_{xt}) \tag{2.3b}$$

The next step is to consider the linear long wave approximations,

$$P_t+ghS_x\approx 0 \tag{2.4a}$$

$$Q_t+ghS_y\approx 0 \tag{2.4b}$$

By spatial differentiation these equations lead to the approximations

$$P_{xxt}+2gh_xS_{xx}+ghS_{xxx}\approx 0 \tag{2.5a}$$

$$P_{xyt}+gh_xS_{xy}+gh_yS_{xx}+ghS_{xxy}\approx 0 \tag{2.5b}$$

$$Q_{yyt}+2gh_yS_{yy}+ghS_{yyy}\approx 0 \tag{2.5c}$$

$$Q_{xyt}+gh_yS_{xy}+gh_xS_{yy}+ghS_{yyx}\approx 0 \tag{2.5d}$$

It is a classical procedure to simplify higher order terms in the Boussinesq or KdV equations by introducing eqs. (2.4a and b) or eqs. (2.5a–d) (see e.g. Mei, 1983). As an example P_{xxt} type terms can be replaced by S_{xxx} type terms by the use of this method. In shallow water it makes no difference, but in deeper water the form of the Boussinesq terms is critical for the accuracy of the linear dispersion relation.

The new Boussinesq equations will now be derived by using the method introduced in Part 1 of this work: We multiply eqs. (2.5a–d) with $-Bh^2$ and add eqs. (2.5a) and (2.5d) to ψ_1 defined in eq. (2.3a), while eqs. (2.5b) and (2.5c) are added to ψ_2 defined in eq. (2.3b). This leads to

$$\begin{aligned}\psi_1 = &-(B+\tfrac{1}{3})h^2(P_{xxt}+Q_{xyt})-Bgh^3(S_{xxx}+S_{xyy})\\ &-hh_x(\tfrac{1}{3}P_{xt}+\tfrac{1}{6}Q_{yt}+2BghS_{xx}+BghS_{yy})-hh_y(\tfrac{1}{6}Q_{xt}+BghS_{xy})\end{aligned} \tag{2.6a}$$

$$\begin{aligned}\psi_2 = &-(B+\tfrac{1}{3})h^2(Q_{yyt}+P_{xyt})-Bgh^3(S_{yyy}+S_{xxy})\\ &-hh_y(\tfrac{1}{3}Q_{yt}+\tfrac{1}{6}P_{xt}+2BghS_{yy}+BghS_{xx})-hh_x(\tfrac{1}{6}P_{yt}+BghS_{xy})\end{aligned} \tag{2.6b}$$

Except for the slope terms proportional to h_x and h_y these expressions are identical to the Boussinesq terms presented in Part 1. Here the value of the coefficient B was determined by matching the resulting linear dispersion relation with a polynomial expansion of Stokes first order theory combined with the use of Pade's approximant. By this approach the value $B=1/15$ was found and the resulting phase celerity was shown to be in excellent agreement with Stokes first order theory for h/L_0 as large as 0.5 (see Fig. 1 in Madsen et al., 1991a).

3. A LINEAR SHOALING ANALYSIS

In this section we shall make a linear shoaling analysis of the new Boussinesq equations. For this purpose we consider the linearized one-dimensional version of eqs. (2.1a–c) combined with eqs. (2.6a and b), which yields

$$S_t+P_x=0 \tag{3.1a}$$

$$P_t+ghS_x-Bgh^3S_{xxx}-(B+\tfrac{1}{3})h^2P_{xxt}-h_x(2Bgh^2S_{xx}+\tfrac{1}{3}hP_{xt})=0 \tag{3.1b}$$

The corresponding wave equation is derived by replacing P_x with $-S_t$ by the use of eq. (3.1a), and by cross-differentiating and subtracting eqs. (3.1a) and (3.1b). This leads to

$$\begin{aligned}&S_{tt}-ghS_{xx}+Bgh^3S_{xxxx}-(B+\tfrac{1}{3})h^2S_{xxtt})=\\ &=h_x(gS_x+(2B+1)hS_{xtt}-5Bgh^2S_{xxx})\end{aligned} \tag{3.2}$$

We shall look for solutions of the form

$$S(x,t)=A(x)e^{i(\omega t-\phi(x))} \tag{3.3}$$

where ω is the cyclic frequency, A is the local wave amplitude and φ is the phase function, which is related to the local wave number by

$$\varphi_x=k(x) \tag{3.4}$$

where the subscript denotes differentiation with respect to x. The water depth, the wave number and the wave amplitude are considered to be slowly varying functions of x, and consequently products of derivatives and higher derivatives of these quantities will be neglected in the following.

The next step is to insert eq. (3.3) into eq. (3.2). To the lowest order all x-derivatives of h, k and A are neglected and we obtain the linear dispersion relation

$$-\omega^2+ghk^2+Bgh^3k^4-(B+\tfrac{1}{3})k^2h^2\omega^2=0 \tag{3.5a}$$

which leads to

$$\frac{c^2}{gh}=\frac{1+Bk^2h^2}{1+(B+\frac{1}{3})k^2h^2} \tag{3.5b}$$

where c is the wave celerity defined by $c=\omega/k$. Collecting terms to the next order in eq. (3.2) includes the terms proportional to the first derivatives of h, k and A and we get

$$\begin{aligned}&A_x(2ghk+4Bgh^3k^3-2(B+\tfrac{1}{3})h^2\omega^2k)+k_x(ghA+6Bgh^3k^2A\\&\quad-(B+\tfrac{1}{3})h^2\omega^2A)+h_x(gkA-(2B+1)h\omega^2kA+5Bgh^2k^3A)=0\end{aligned} \tag{3.6}$$

The frequency ω is eliminated from eq. (3.6) by the use of eq. (3.5a) and after algebraic manipulations we get

$$\alpha_1\frac{A_x}{A}+\alpha_2\frac{k_x}{k}+\alpha_3\frac{h_x}{h}=0 \tag{3.7}$$

where

$$\alpha_1\equiv 2(1+2Bk^2h^2+B(B+\tfrac{1}{3})k^4h^4) \tag{3.8a}$$

$$\alpha_2\equiv 1+6Bk^2h^2+5B(B+\tfrac{1}{3})k^4h^4 \tag{3.8b}$$

$$\alpha_3\equiv 1+(4B-\tfrac{2}{5})k^2h^2+B(3B+\tfrac{2}{5})k^4h^4 \tag{3.8c}$$

The remaining step is to express k_x/k in terms of h_x/h. Such a relation can be derived by differentiation of the linear dispersion relation (3.5a). Again we eliminate ω from the expressions and obtain the solution

$$\frac{k_x}{k}=-\alpha_4\frac{h_x}{h} \tag{3.9}$$

where

$$\alpha_4 \equiv \tfrac{1}{2}\left[\frac{1+(2B-\frac{1}{3})k^2h^2+B(B+\frac{1}{3})k^4h^4}{1+2Bk^2h^2+B(B+\frac{1}{3})k^4h^4}\right] \tag{3.10}$$

Finally eq. (3.9) is inserted into eq. (3.7), which is solved with respect to A_x/A and the resulting linear shoaling equation becomes

$$\frac{A_x}{A} = -\alpha_5 \frac{h_x}{h} \tag{3.11}$$

where

$$\alpha_5 \equiv \frac{\alpha_3 - \alpha_2\alpha_4}{\alpha_1} \tag{3.12}$$

For reference we shall determine expressions for α_4 and α_5 based on Stokes first order theory. In this case the shoaling equation is derived by using the concept of energy flux conservation, which can be expressed by

$$\frac{\partial}{\partial x}(A^2C_g) = 0 \tag{3.13}$$

Here C_g is the group velocity defined by

$$C_g = \tfrac{1}{2}(1+G)C \tag{3.14}$$

where

$$G \equiv \frac{2kh}{\sin 2kh} \tag{3.15}$$

and from the definition of C we find that C_x/C is equal to $-k_x/k$. Hence eq. (3.13) can be expressed by

$$\frac{A_x}{A} = \tfrac{1}{2}\left(\frac{k_x}{k} - \frac{G_x}{1+G}\right) \tag{3.16}$$

Again the relative change of the wave number is determined by differentiation of the linear dispersion relation, which leads to eq. (3.9) with α_4 defined by

$$\alpha_4^{\text{stokes}} = \frac{G}{1+G} \tag{3.17}$$

Finally eqs. (3.9), (3.15) and (3.17) can be inserted in eq. (3.16) and after algebraic manipulations we obtain eq. (3.11) with α_5 defined by

$$\alpha_5^{\text{stokes}} = \frac{G(1+\frac{1}{2}G(1-\cosh 2kh)}{(1+G)^2} \tag{3.18}$$

In shallow water, i.e. for $kh \to 0$, a Taylor expansion leads to

$$\alpha_4^{\text{stokes}} \to \tfrac{1}{2}(1 - \tfrac{1}{3}k^2h^2 + \cdots) \tag{3.19a}$$

$$\alpha_5^{\text{stokes}} \to \tfrac{1}{4}(1 - k^2h^2 + \cdots) \tag{3.19b}$$

and this can be shown to agree with the shallow water approximation to the Boussinesq expressions (3.10) and (3.12) for arbitrary values of the linear dispersion coefficient B. On the other hand eqs. (3.10) and (3.12) simplify to eqs. (3.19a and b) for arbitrary wave numbers for the case of $B=0$ (standard Boussinesq equations).

In Fig. 1 the variation of the shoaling gradient α_5 is shown as a function of h/L_0. This requires that eq. (3.12) is combined with a solution of the Boussinesq dispersion relation from eq. (3.5a), while eq. (3.18) is combined with Stokes dispersion relation. It can be concluded that the standard Boussinesq equations with $B=0$ lead to major discrepancies for h/L_0 larger than 0.10, while $B=1/15$ has a remarkable effect and results in an excellent agreement with Stokes first order theory for h/L_0 as large as 0.50.

In Part 1 of this work we neglected the Boussinesq terms proportional to h_x in the momentum equation (3.1b) with the argument of considering a mildly sloping sea bed. Unfortunately, however, the effect of these terms can be shown to be accumulative and they have a major influence on the shoaling properties

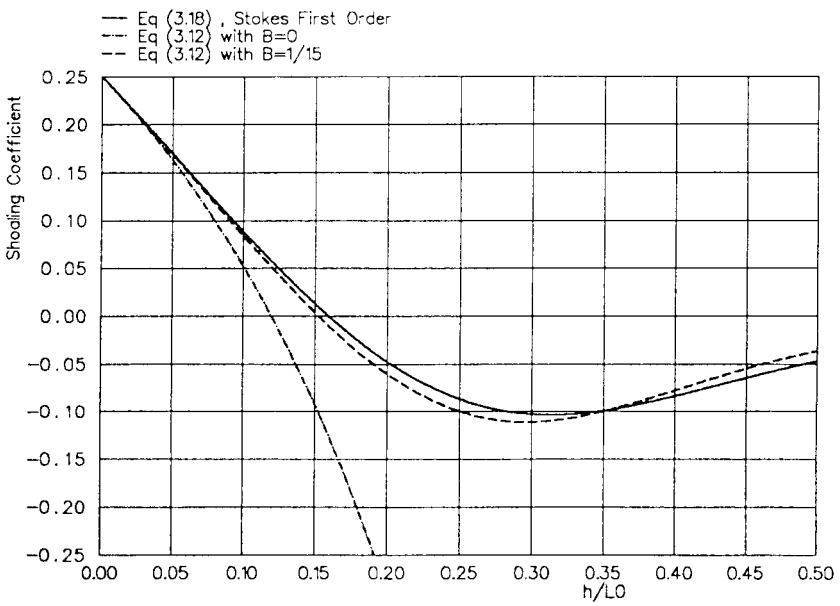

Fig. 1. Linear shoaling gradient, α_5 defined by the relation $A_x/A = -\alpha_5 h_x/h$.

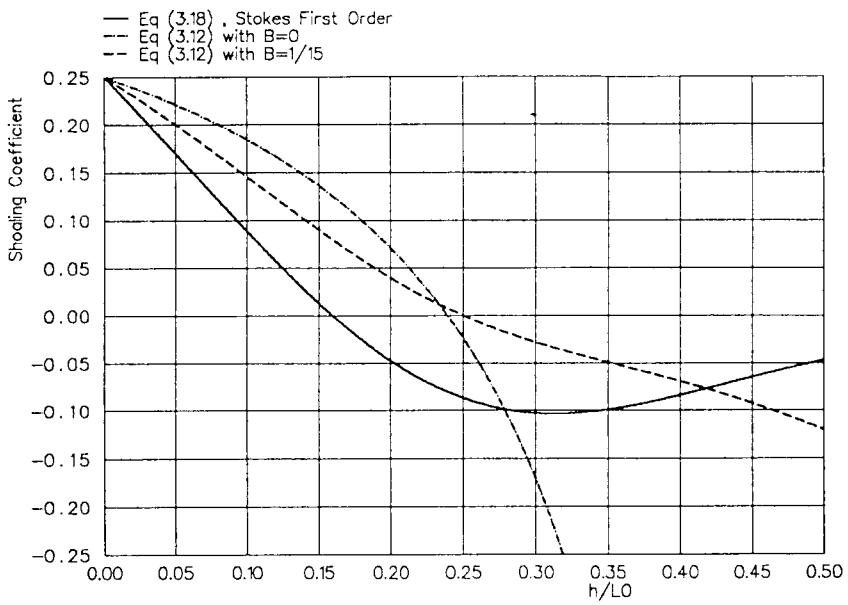

Fig. 2. Linear shoaling gradient, α_5 when Boussinesq terms proportional to h_x in the momentum equation are neglected.

of the equations. If these terms are neglected in eq. (3.1b) the coefficient α_3 defined in eq. (3.8c) is changed to

$$\alpha_3^* = 1 + (2B - \tfrac{1}{3})k^2h^2 + B(B + \tfrac{1}{3})k^4h^4 \tag{3.20}$$

and the effect on the shoaling gradient α_5 is shown in Fig. 2. The result is seen to be a considerable overestimation of the shoaling gradient.

4. THE NUMERICAL SCHEME

In this section we shall specify the finite difference representation of the governing equations (2.1a–c) with the new Boussinesq terms defined by eqs. (2.6a and b). The presentation includes a specification of the nonlinear convective terms, which were not described in Part 1, and introduces an improved time centering of the cross-Boussinesq terms.

As explained in Part 1 the differential equations are discretized by using a time-centered implicit scheme with variables defined on a space-staggered rectangular grid. The method is based on the ADI (Alternating Direction Implicit) algorithm, and the resulting system of finite difference equations is reduced to a three-diagonal system, which is solved by the Double Sweep algorithm.

In order to emphasize the time-centering of the terms, the x- and y-deriva-

tives will be given in their differential form only. The finite-difference approximation of the spatial derivatives is a straight forward mid-centering except for the nonlinear convective terms, which are described in detail at the end of this section. The resulting x-sweep equations read:

$$\left(\frac{S^{n+1/2}-S^n}{\frac{1}{2}\Delta t}\right)+\tfrac{1}{2}(P_x^{n+1}+P_x^n)+\tfrac{1}{2}(Q_y^{n+1/2}+Q_y^{n-1/2})=0 \tag{4.1a}$$

$$\left(\frac{P^{n+1}-P^n}{\Delta t}\right)+\left(\frac{P^2}{d}\right)_x^{n+1/2}+\left(\frac{PQ}{d}\right)_y^{n+1/2}+gd^*S_x^{n+1/2}$$

$$-(B+\tfrac{1}{3})\frac{h^2}{\Delta t}[(P_{xx}^{n+1}-P_{xx}^n)+\tfrac{3}{2}(Q_{xy}^{n+1/2}-Q_{xy}^{n-1/2})-\tfrac{1}{2}(Q_{xy}^{n-1/2}$$

$$-Q_{xy}^{n-3/2})]-\frac{hh_x}{\Delta t}[\tfrac{1}{3}(P_x^{n+1}-P_x^n)+\tfrac{1}{4}(Q_y^{n+1/2}-Q_y^{n-1/2})-\tfrac{1}{12}(Q_y^{n-1/2}$$

$$-Q_y^{n-3/2})]-\frac{hh_y}{\Delta t}[\tfrac{1}{4}(Q_x^{n+1/2}-Q_x^{n-1/2})-\tfrac{1}{12}(Q_x^{n-1/2}-Q_x^{n-3/2})]$$

$$-Bgh^2[h(S_{xxx}^*+S_{xyy}^*)+h_x(2S_{xx}^*+S_{yy}^*)+h_yS_{xy}^*]=0 \tag{4.1b}$$

in which $S^{n+1/2}$ and P^{n+1} are the unknown variables. The resulting y-sweep equations read:

$$\left(\frac{S^{n+1}-S^{n+1/2}}{\frac{1}{2}\Delta t}\right)+\tfrac{1}{2}(P_x^{n+1}+P_x^n)+\tfrac{1}{2}(Q_y^{n+3/2}+Q_y^{n+1/2})=0 \tag{4.2a}$$

$$\left(\frac{Q^{n+3/2}-Q^{n+1/2}}{\Delta t}\right)+\left(\frac{Q^2}{d}\right)_y^{n+1}+\left(\frac{PQ}{d}\right)_x^{n+1}+gd^{**}S_y^{n+1}$$

$$-(B+\tfrac{1}{3})\frac{h^2}{\Delta t}[(Q_{yy}^{n+3/2}-Q_{yy}^{n+1/2})+\tfrac{3}{2}(P_{xy}^{n+1}-P_{xy}^n)-\tfrac{1}{2}(P_{xy}^n-P_{xy}^{n-1})]$$

$$-\frac{hh_y}{\Delta t}[\tfrac{1}{3}(Q_y^{n+3/2}-Q_y^{n+1/2})+\tfrac{1}{4}(P_x^{n+1}-P_x^n)-\tfrac{1}{12}(P_x^n-P_x^{n-1})]$$

$$-\frac{hh_x}{\Delta t}[\tfrac{1}{4}(P_y^{n+1}-P_y^n)-\tfrac{1}{12}(P_y^n-P_y^{n-1})]-Bgh^2[h(S_{yyy}^{**}+S_{yxx}^{**})$$

$$+h_y(2S_{yy}^{**}+S_{xx}^{**})+h_xS_{xy}^{**}]=0 \tag{4.2b}$$

in which S^{n+1} *and* $Q^{n+3/2}$ are the unknown variables. The * used in eq. (4.1b) and ** used in eq. (4.2b) indicate estimated values of the unknown surface elevation at time levels $n+1/2$ and $n+1$, respectively. As mentioned in Part 1 these values are calculated by explicit use of the continuity equation and by doing so the nonlinear gravity term and the convective terms can be time-centered without using iteration. Furthermore these estimated surface eleva-

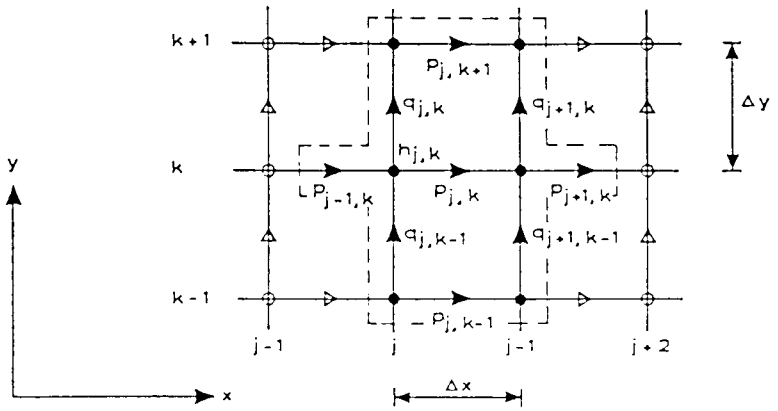

Fig. 3. Grid notation used for x-momentum equation.

tions are used to determine the new Boussinesq terms S_{xxx}, S_{xyy}, S_{yyy}, S_{yxx}, S_{xx}, S_{yy} and S_{xy}. This technique however requires a relatively fine resolution of the wave period in order to avoid artificial dissipation of the wave energy, a problem which will be enhanced for increasing values of h/L_0. It turns out that a resolution of 24–30 time steps per period is necessary in deep water, while the wave length resolution can be restricted to 8–10 grid points.

The representation of the cross-Boussinesq terms (i.e. Q_{xyt}, Q_{yt} and Q_{xt} in the x-sweep and P_{xyt}, P_{xt} and P_{yt} in the y-sweep) has required special attention and in order to obtain the correct time-centering we have used linear time-extrapolation of these terms. A straight forward representation, like the one presented in Part 1, leads to a backward centering (half a time step) of these terms and this will result in artificial dissipation of waves propagating with an angle to the grid. Again this effect will be enhanced for increasing values of h/L_0, and the extrapolation used to avoid it requires a fine resolution of the wave period.

The representation of the nonlinear convective terms is described in detail below. Referring to the notation of Fig. 3 the x-sweep contributions are described by

$$\left(\frac{P^2}{d}\right)_x = \left[\left(\frac{P^{n+1}_{j,k}+P^{n+1}_{j+1,k}}{2}\right)\left(\frac{P^{n}_{j,k}+P^{n}_{j+1,k}}{2}\right)\frac{1}{d^*_{j+1,k}} - \left(\frac{P^{n+1}_{j,k}+P^{n+1}_{j-1,k}}{2}\right)\left(\frac{P^{n}_{j,k}+P^{n}_{j-1,k}}{2}\right)\frac{1}{d^*_{j,k}}\right]\frac{1}{\Delta x} \tag{4.3a}$$

$$\left(\frac{PQ}{d}\right)_y = \left[\left(\frac{P^{a}_{j,k+1}+P^{b}_{j,k}}{2}\right)V^{n+1/2}_{j+1/2,k+1/2} - \left(\frac{P^{a}_{j,k}+P^{b}_{j,k-1}}{2}\right)V^{n+1/2}_{j+1/2,k-1/2}\right]\frac{1}{\Delta y} \tag{4.3b}$$

where

$$V^{n+1/2}_{j+1/2,k+1/2}=\frac{2(Q^{n+1/2}_{j,k}+Q^{n+1/2}_{j+1,k})}{(d^{*}_{j,k}+d^{*}_{j,k+1}+d^{*}_{j+1,k}+d^{*}_{j+1,k+1})} \tag{4.4a}$$

$$V^{n+1/2}_{j+1/2,k-1/2}=\frac{2(Q^{n+1/2}_{j,k-1}+Q^{n+1/2}_{j+1,k-1})}{(d^{*}_{j,k-1}+d^{*}_{j,k}+d^{*}_{j+1,k-1}+d^{*}_{j+1,k})} \tag{4.4b}$$

The cross-momentum term, eq. (4.3b), is time-centered by the use of the so-called "side-feeding" technique, where every second x-sweep is performed in the positive y-direction ("up"-sweep) in which case $a=n$ and $b=n+1$, and the remaining x-sweeps are performed in the negative y-direction ("down"-sweep) in which case $a=n+1$ and $b=n$. Again the * used in eqs. (4.3) and (4.4) indicates estimated values of the water depth at time level $n+\frac{1}{2}$.

Finally it should be mentioned that the treatment of open boundaries was discussed in Part 1. Here we shall only repeat that surface elevation boundaries require that S as well as S_{xx} (the curvature) is specified and flux boundaries require that P as well as S_x (the gradient) is specified.

5. VERIFICATION WITH RESPECT TO LINEAR SHOALING

In order to verify the linear shoaling properties of the new Boussinesq model the following test case has been studied: At the seaward (western) boundary the water depth is 13 m. The bottom is flat for the first 10 m distance from the boundary while it has a constant slope of 1/50 from 10 m to 650 m distance. Finally from 650 m to 700 m the bottom is flat again with a water depth of 0.2 m. All nonlinear terms in the Boussinesq equations are switched off, the coefficient B is set to 1/15, and the grid size and time step are chosen to be 1.0 m and 0.08 s, respectively. The shoreward (eastern) boundary is covered by a 50 point wide absorbing sponge layer, while time series of S (surface elevation) and S_{xx} (the curvature of S) are specified at the open western boundary.

As a typical deep water example we have chosen the wave period of 4.0 s leading to a variation of h/L_0 from 0.52 to 0.008. A sequence of line plots of the computed surface elevation, covering one wave period, is shown in Fig. 4a while Fig. 4b shows a comparison between the computed maximum elevations and the shoaling curve obtained from Stokes first order theory. The agreement is seen to be most satisfactory with relative errors less than 3% everywhere. The similar comparison is made in Fig. 5a and b for the wave period of 8.0 s, which is a typical shallow water example leading to the h/L_0 variation of 0.13 to 0.002. Again the accuracy of the simulation is most satisfactory.

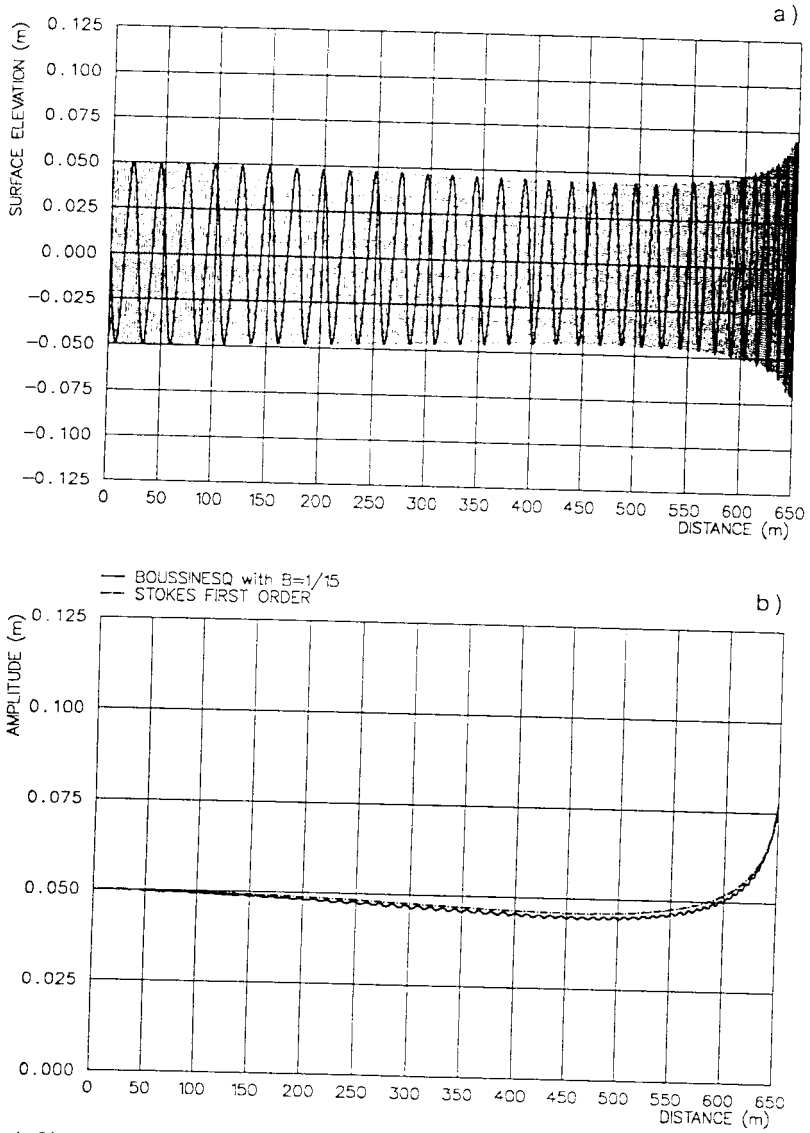

Fig. 4. Simulation of linear shoaling from deep to shallow water. Wave period = 4.0 s, water depth = 13–0.2 m, $B = 1/15$. (a) Envelope of computed surface elevations. (b) Maximum elevations compared to Stokes first order theory.

The absorbing sponge layer at the eastern boundary is extremely efficient and practically no reflections occur in simulations made on a horizontal bottom. Hence the small oscillations in Figs. 4b and 5b are due to reflections from the sloping beach.

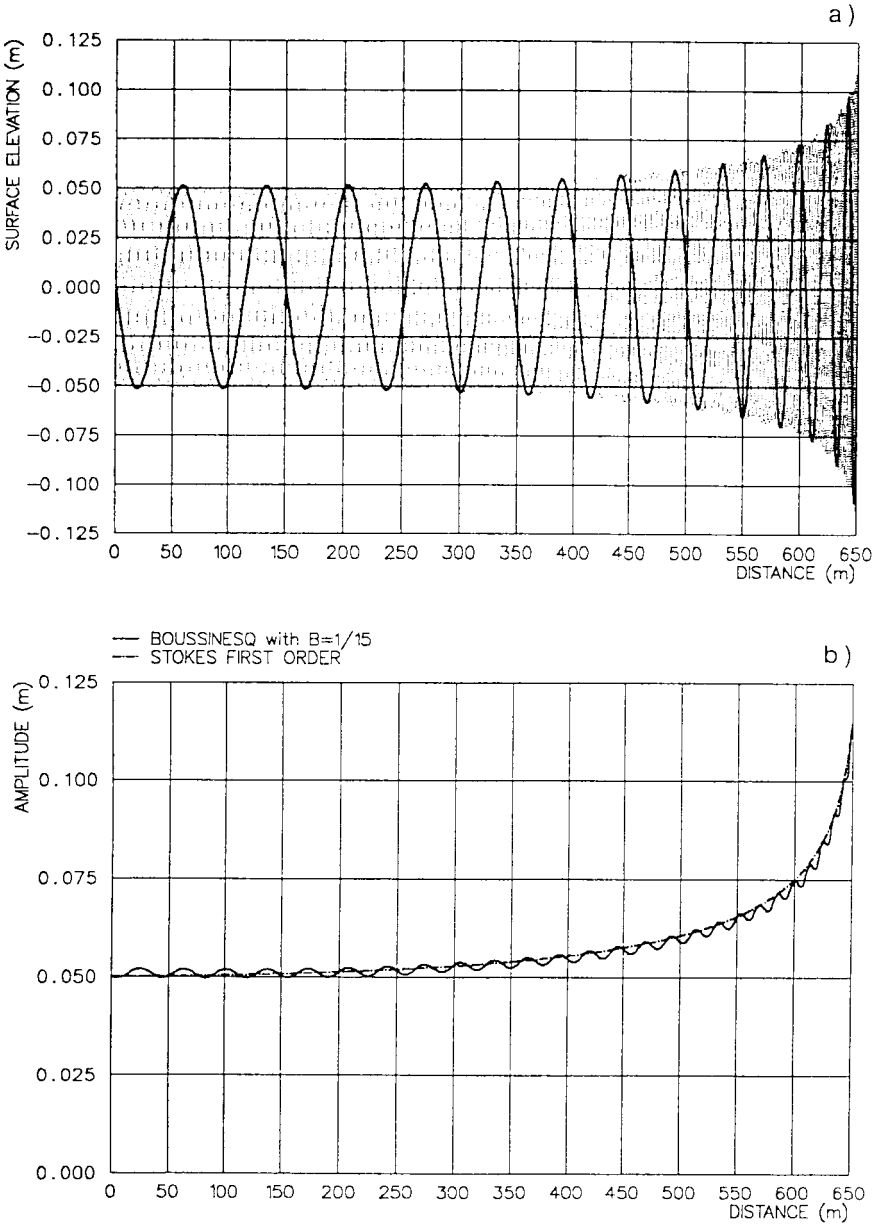

Fig. 5. Simulation of linear shoaling from intermediate to shallow water. Wave period = 8.0 s, water depth = 13–0.2 m, $B = 1/15$. (a) Envelope of computed surface elevations. (b) Maximum elevations compared to Stokes first order theory.

6. VERIFICATION WITH RESPECT TO NONLINEAR REFRACTION-DIFFRACTION

Nonlinear refraction–diffraction over a semicircular shoal was studied experimentally by Whalin (1971) for waves in deep, intermediate and shallow water. The topography used by Whalin can be described by

$$h(x,y)=\begin{cases}0.4572 & (0\le x\le 10.67-G)\\ 0.4572+\frac{1}{25}(10.67-G-x) & (10.67-G\le x\le 18.29-G)\\ 0.1524 & (18.29-G\le x\le 21.34)\end{cases}$$

$$G(y) = [y(6.096-y)]^{1/2} \qquad (0\le y\le 6.096)$$

where the length variables x and y are measured in meters. The topography is symmetric with respect to the centreline at $y=3.048$ m, the width is 6.096 m and the water depth varies from 0.457 m to 0.152 m. Whalin conducted three sets of experiments by generating waves in the deeper part of the model with periods of 1, 2 and 3 seconds. In Table 1 the experimental information is summarized. At the wave maker the waves are linear but after the focusing on the shoal higher harmonics become significant due to nonlinear effects.

Previous numerical studies of this experiment have been presented by Liu and Tsay (1984), Liu et al. (1985) and Rygg (1988). Liu and Tsay (1984) derived a set of nonlinear Schrödinger equations to describe the amplitude evolution of second order Stokes waves propagating in a single direction over a slowly varying bathymetry. Their numerical model was applicable for small values of the Ursell parameter and comparisons were made with the Whalin's experiments for the wave periods of 1 and 2 seconds. Liu et al. (1985) studied the case of $T=3$ seconds by using the classical Boussinesq equations to derive evolution equations for spectral-wave components in a slowly varying two-

TABLE 1

Experimental information at water depth $h=0.4562$ m

Wave period (s)	Wave amplitude (m)	h/L_0	$\frac{(a/h)}{(kh)^2}$
1.0	0.0097	0.29	0.0058
1.0	0.0195	0.29	0.0116
2.0	0.0075	0.073	0.0304
2.0	0.0106	0.073	0.0429
2.0	0.0149	0.073	0.0604
3.0	0.0068	0.033	0.0682
3.0	0.0098	0.033	0.0983
3.0	0.0146	0.033	0.1464

dimensional domain. Finally, Rygg (1988) presented time-domain solutions to the classical Boussinesq equations for wave periods of 2 and 3 seconds.

The new formulation of the Boussinesq equations presented in this paper makes it possible to consider all three sets of Whalin's experiments with 1, 2 and 3 second waves. We shall concentrate on a discussion of the case of 1 second waves, since this has not previously been treated by the use of Boussinesq equations. We start the discussion by considering one-dimensional simulations with pure shoaling along the centreline of the Whalin's bathymetry (i.e. at $y=3.048$ m). In this case the value of h/L_0 varies from 0.29 in front of the shoal to 0.096 behind the shoal. The minimum wave length becomes approximately 1.10 m and in order to achieve a reasonable resolution a grid size of 0.0762 m and a timestep of 0.01953 s have been chosen. At the seaward boundary (at $x=0$) time series of S (surface elevation) and S_{xx} (the curvature of S) are specified. A 50 point wide absorbing sponge layer covers the region from $x=30$ m to $x=34$ m.

Simulations are made with the new Boussinesq equations (with $B=1/15$) covering a period of 78 s, which allows possible reflections to develop in the

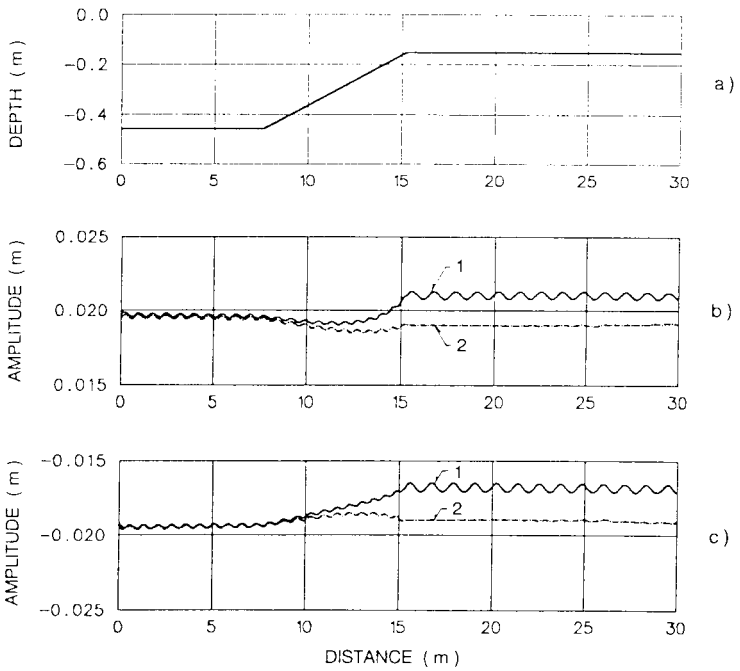

Fig. 6. Linear and nonlinear shoaling along the centre line of Whalin's bathymetry (at $y=3.048$ m). Period = 1.0 s, amplitude = 0.0195 m, grid size = 0.0762 m, time step = 0.01953 s, Boussinesq equation with $B=1/15$. 1: Nonlinear equations. 2: Linearized equations. (a) Topography. (b) Maximum elevations of the wave envelope. (c) Minimum elevations of the wave envelope.

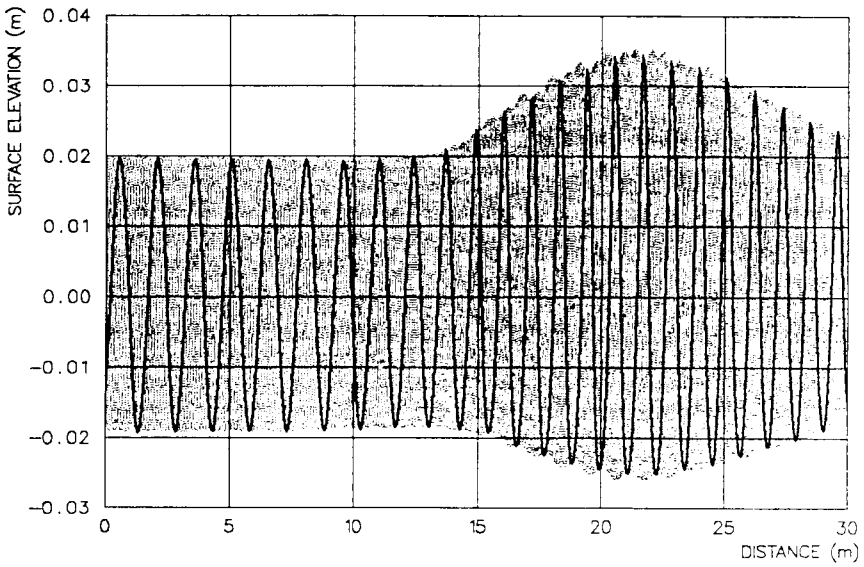

Fig. 7. Refraction–diffraction in Whalin's bathymetry. Results presented as envelope of surface elevations along the centre line (at $y=3.048$ m). Period $=1.0$ s, amplitude $=0.0195$ m, grid size $=0.0762$ m, timestep $=0.01953$ s, Boussinesq equation with $B=1/15$.

model area. In Fig. 6 the maximum and minimum values of the resulting envelope of computed surface elevations are presented. For the case of linear shoaling (i.e. with all nonlinear terms switched off in the Boussinesq equations) we notice that practically no reflections occur on the shallow shelf which proves the efficiency of the absorbing sponge layer. Reflections do occur on the seaward side of the shoal for $x \leqslant 15$ m, and the beat length in the wave envelope is 0.76 m, which is in perfect agreement with half a wave length. The case of nonlinear shoaling is practically identical with the linear shoaling for $x \leqslant 12$ m but clear differences occur on the shelf area for $x > 15$ m: the maximum and minimum levels in the envelope are raised and oscillations occur with a beat length of 1.14 m. These oscillations are not caused by reflections but are due to interactions between bound second harmonics travelling with the primary wave and free second harmonics travelling with their own speed. The release of free second harmonics during the process of shoaling has previously been discussed by e.g. Mei (1983) and it can be concluded that if in a horizontal part a permanent wave is present, with no free harmonics, the shoaling due to depth-variations can destroy the permanency and free harmonics can be generated (see also Liu, 1989). On a horizontal bottom this phenomenon is known to occur if linear monochromatic boundary conditions are applied in shallow water in which case a significant amount of free second harmonic energy will be released. The resulting modulation of the wave

train has been analyzed by e.g. Mei and Ünlüata (1972) and Bryant (1973) and a discussion of the capability of the new Boussinesq equations to describe these phenomena can be found in Madsen et al. (1991b), and Madsen and Sørensen (1992). Simulations made on a constant depth of 0.15 m confirm the beat length of 1.14 m found in Fig. 6.

We shall now return to the two-dimensional refraction–diffraction problem and Fig. 7 presents the computed envelope of surface elevations along the centreline for the case of 1 second waves. A comparison with Fig. 6 shows the strong focusing effect, which becomes important behind the shoal and a major increase in amplitudes is observed. The modulation of the envelope has also increased and now the two wave systems (of bound and free harmonics) will propagate not only with different speeds but also with different directions. The bound second harmonics will follow the primary wave (with $h/L_0=0.096$ on the shelf) towards the focusing spot, while the free second harmonics (with $h/L_0=0.38$) will pass the shoal almost without any change in direction. This will lead to a complicated modulation pattern as seen from the perspective plot of the maximum elevations in Fig. 8.

An FFT analysis of time series in each grid point along the centreline has

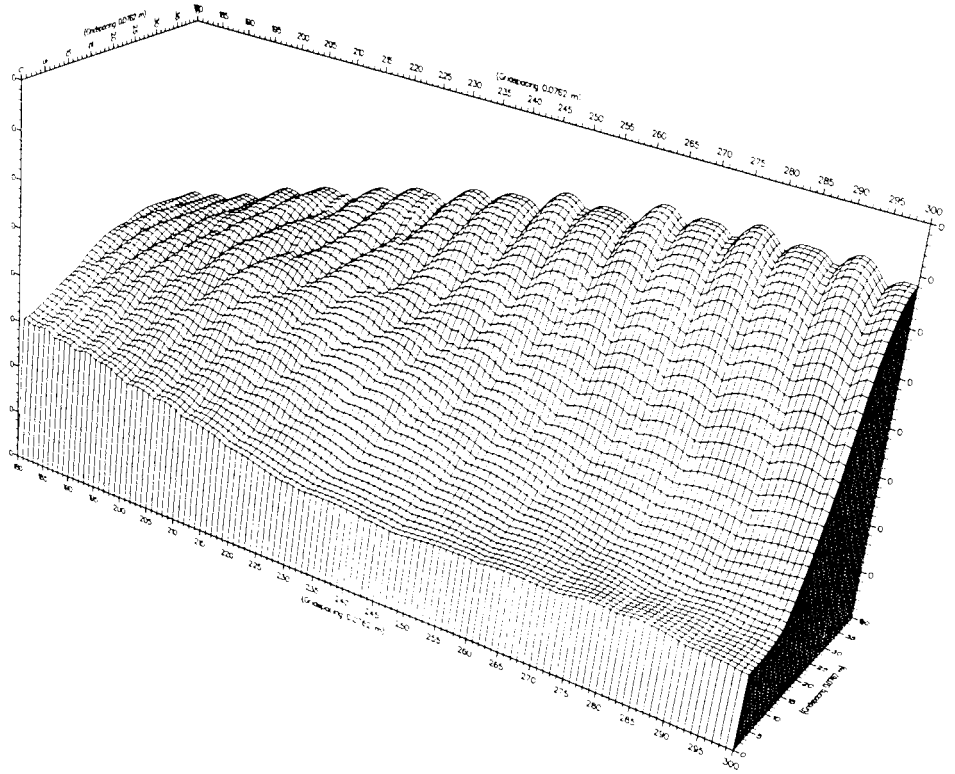

Fig. 8. Perspective plot of maximum surface elevations in wave envelope (data as in Fig. 7).

been made and the resulting spatial evolution of first and second harmonics is compared with Whalin's experimental data in Fig. 9. A considerable scattering in the data is seen in front of the shoal but behind the shoal the agreement between the data and the Boussinesq results is acceptable: The first harmonic is slightly overestimated while the second harmonic is slightly underestimated. For the purpose of comparison Fig. 9 also includes the results obtained by Liu and Tsay (1984) using the nonlinear Schrödinger equation. Their results slightly overestimate the second harmonic as well as the first harmonic. Compared to the Boussinesq equations the second harmonic is clearly higher while the first harmonic is almost identical except for a region far behind the focusing area. An explanation for the discrepancy in the second harmonic can be given by considering regular 1 second waves with a wave height of 0.06 m at the water depth of 0.1524 m: Stokes second order theory (which corresponds to the approach by Liu and Tsay) leads to a first harmonic of 0.03 m and a second harmonic of 0.0096 m, while Fourier solutions to the Boussinesq equations (see Madsen and Sørensen, 1992) lead to a second harmonic of 0.0065 m. These numbers are in qualitative agreement with the computed conditions at the focus point at $x=21$ m. The data by Whalin is seen to be scattered in the interval between the two different model results. The oscillations in the second harmonics obtained by the present model once again are an indication of the combination of bound and free harmonics. From

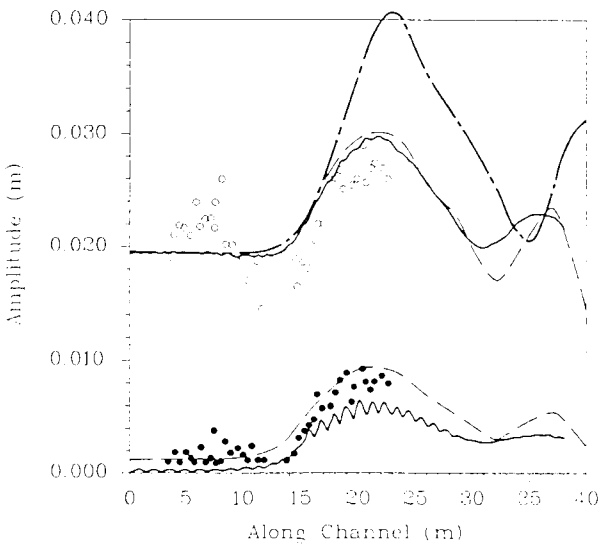

Fig. 9. Wave amplitudes for the first and second harmonic along the centre line (period = 1.0 s, amplitude = 0.0195 m). (○), (●) Measured first and second harmonic amplitudes (Whalin, 1971), {——} Boussinesq equation with $B=1/15$, (— —) results by Liu and Tsay (1984), (-·-) results by Lozano and Liu (1980).

the data of Whalin we cannot conclude whether the simulated modulations should be there or not, and the results by Liu and Tsay do not contain oscillations simply because their equation does not allow for harmonic interactions. Finally Fig. 9 also includes the linear solution presented by Lozano and Liu (1980). This leads to a major overestimation of the first harmonic as well as of the focusing effect on the wave height.

The test case with 1 second waves has been repeated by using the standard Boussinesq equations ($B=0$) and the result is compared with the new Boussinesq equations in Fig. 10. The effect is seen to be dramatic and the result obtained by using $B=0$ is quite useless. The significant and unrealistic decrease of the first harmonic from $x=7.62$ m to $x=15$ m can be explained as pure shoaling falsification: The linear shoaling gradients were shown in Fig. 1 and spatial integration from $h/L_0=0.29$ at the toe of the shoal to $h/L_0=0.096$ at the top leads to a 25% decrease in wave height with $B=0$. With $B=1/15$ (and with the exact linear shoaling curve) the wave height is reduced with 3% in the first part of the slope, increased with a similar amount in the second part and at the top it is then approximately the same as it was at the toe of the slope (see also Fig. 6).

In fact this example demonstrates that Fig. 1 should be taken quite seriously as a measure of the range of application of different types of Boussinesq equations. Very often the accuracy of the wave celerity is taken as the practical measure, in which case a 5% error restricts the use of the standard Bous-

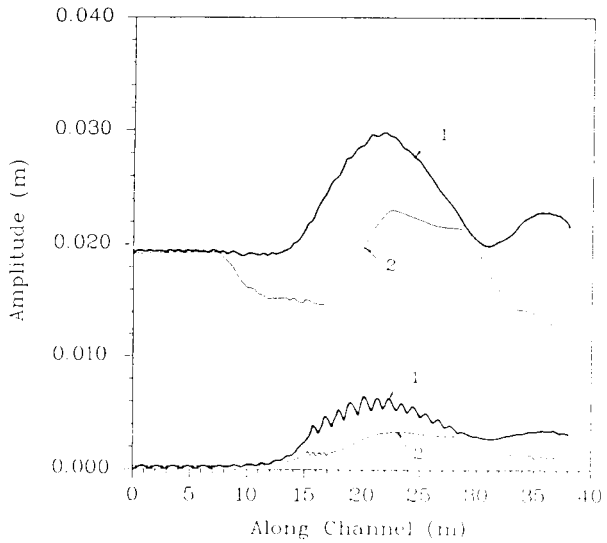

Fig. 10. Comparison with standard Boussinesq equations (data as Fig. 7). 1: New Boussinesq equation with $B=1/15$, 2: standard Boussinesq equation, i.e. $B=0$.

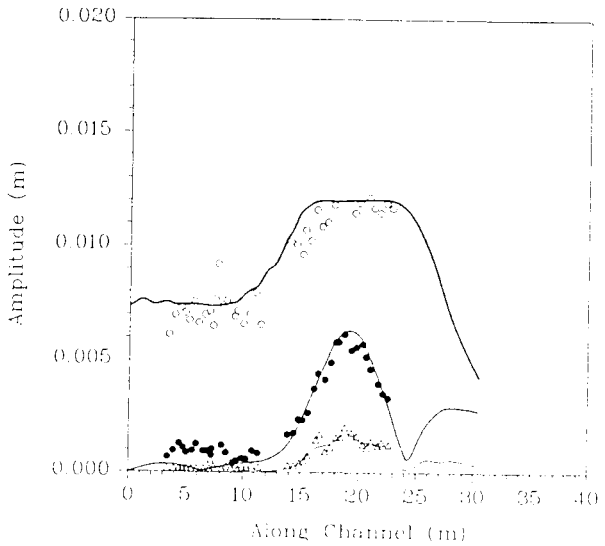

Fig. 11. Wave amplitudes for the first, second and third harmonic along the centre line (period = 2.0 s, amplitude = 0.0075 m). (○), (●), (△) Measured harmonic amplitudes (Whalin, 1971), {——} Boussinesq equation with $B = 1/15$ (grid size 0.1524 m, time step 0.03906 s).

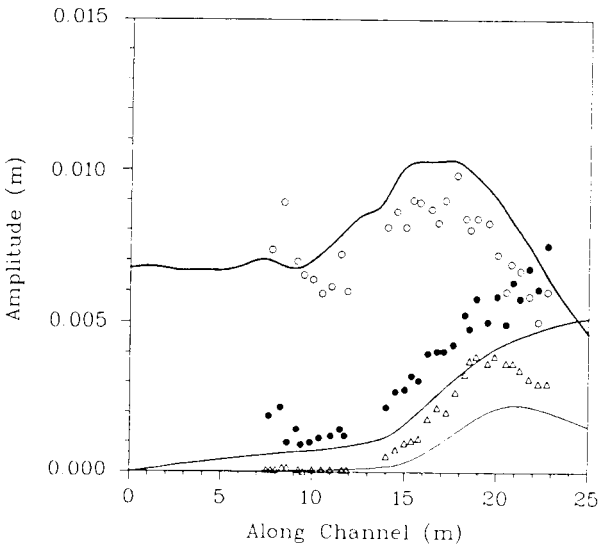

Fig. 12. Wave amplitudes for the first, second and third harmonic along the centre line (period = 3.0 s, amplitude = 0.0068 m). (○), (●), (△) Measured harmonic amplitudes (Whalin, 1971), {——} Boussinesq equation with $B = 1/15$ (grid size 0.1524 m, time step 0.03516 s).

sinesq equations to approximately $h/L_0=0.22$. However, according to Fig. 1 this is clearly much too optimistic in case of a variable bathymetry and the shoaling falsification increases rapidly for h/L_0 exceeding 0.12. On the other hand this only emphasizes the importance of using the new Boussinesq equations presented in this paper, in which case h/L_0 as large as 0.5 can be considered.

We finish this chapter on the Whalin experiments by showing a simulation with 2 second waves (Fig. 11) and 3 second waves (Fig. 12). In both cases the agreement with the measurements is most acceptable. The other four shallow water test cases listed in Table 1 have also been simulated, but they will not be reported here, since it can be concluded that for the 2 and 3 second waves the results obtained by the new equations are almost identical to the results by Rygg (1988), who used the classical Boussinesq equations.

7. CONCLUSIONS

The principles from Madsen et al. (1991a) are generalized from a horizontal to a sloping bottom, and this paper presents extended Boussinesq equations applicable to irregular wave propagation on a slowly varying bathymetry from deep to shallow water. The equations incorporate excellent linear dispersion characteristics, which are valuable in shallow water and of the utmost importance in deep water.

The linear dispersion coefficient, B is the key parameter in the new Boussinesq equations. With $B=0$ the standard equations are obtained, while $B=1/15$ is determined from the Pade's approximant technique. In Part 1 (Madsen et al., 1991a) other values of B were discussed and it was suggested to consider B as a curve fitting parameter in the process of obtaining the best overall agreement with Stokes first order theory with respect to phase celerity and group velocity. In the present paper we have decided to consider the value $B=1/15$ for the following reasons:

(a) The Pade's approximant technique gives a physical/mathematical explanation of this choice.

(b) With this value the discrepancies relative to Stokes theory will increase continuously with the value of h/L_0.

(c) With this value an excellent agreement in the shoaling coefficient and the phase celerity is obtained for h/L_0 as large as 0.5.

In Part 1 (Madsen et al., 1991a) the new equations were analyzed and solved for linear wave propagation and diffraction on a horizontal bottom. In this paper we have concentrated on linear shoaling on a constant slope and nonlinear refraction–diffraction on the semicircular shoal of Whalin. The ac-

curacy of the computed results is seen to be most acceptable. Finally it should be mentioned that the nonlinear properties of the new equations is investigated in further detail by Madsen and Sørensen (1992), who present second order boundary conditions for irregular waves and study the phenomena of bound waves and wave–wave interaction in shallow water. Also for this purpose the excellent linear dispersion characteristics of the new equations turn out to be valuable.

REFERENCES

Abbott, M.B., Petersen, H.M. and Skovgaard, O., 1978. On the numerical modelling of short waves in shallow water. J. Hydraul. Res., 16(3): 173–203.

Bryant, P.J., 1973. Periodic waves in shallow water. J. Fluid Mech., 59(4): 625–644.

Liu, P.L.-F., 1989. A note on long waves induced by short-wave groups over a shelf. J. Fluid Mech., 205: 163–170.

Liu, P.L.-F. and Tsay, T.-K., 1984. Refraction–diffraction model for weakly nonlinear water waves. J. Fluid Mech., 141: 265–274.

Liu, P.L.-F., Yoon, S.B. and Kirby, J.T., 1985. Nonlinear refraction–diffraction of waves in shallow water. J. Fluid Mech., 153: 185–201.

Lozano, C. and Liu, P.L.-F., 1980. Refraction–diffraction model for linear surface water waves. J. Fluid Mech., 101: 705–720.

Madsen, P.A., Murray, R. and Sørensen, O.R., 1991a. A new form of the Boussinesq equations with improved linear dispersion characteristics (Part 1). Coastal Eng., 15: 371–388.

Madsen, P.A., Sørensen, O.R. and Yang Zhenyong, 1991b. Wave–wave interaction in shallow water. Proc. XXIV IAHR Congress, Madrid, September 1991, pp. B001–B011.

Madsen, P.A. and Sørensen, O.R., 1992. Bound waves and triad interactions in shallow water. J. Ocean Eng., in press.

McCowan, A.D., 1987. The range of application of Boussinesq type numerical short wave models. Proc. 22nd IAHR Congr., Lausanne.

Mei, C.C. and Ünlüata, U., 1972. Harmonic generation in shallow water waves. In: R.E. Meyer (Editor), Waves on Beaches and Resulting Sediment Transport. Academic Press, New York, pp. 181–202.

Mei, C.C., 1983. The Applied Dynamics of Ocean Surface Waves. Wiley, New York, 740 pp.

Peregrine, D.H., 1967. Long waves on a beach. J. Fluid Mech., 27(4): 815–827.

Rygg, O.B., 1988. Nonlinear refraction–diffraction of surface waves in intermediate and shallow water. Coastal Eng., 12: 191–211.

Whalin, R.W., 1971. The limit of applicability of linear wave refraction theory in a convergence zone. Res. Rep. H-71-3, U.S. Army Corps of Engineers, Waterways Expt. Station, Vicksburg, MS.

Witting, J.M., 1984. A unified model for the evolution of nonlinear water waves. J. Comput. Phys., 56: 203–236.